Cross Sections for Collisions of Electrons and Photons with Atomic Oxygen

Y. Itikawa and A. Ichimura

Institute of Space and Astronautical Science, Yoshinodai, Sagamihara 229, Japan

Received July 5, 1989; revised manuscript received November 26, 1989

Data have been compiled on the cross sections for the collisions of electrons and photons with atomic oxygen (O). The processes considered are total scattering, elastic scattering, momentum transfer, excitations of electronic states (including fine structure levels of the ground state), ionization, and electron attachment. The cross-section data are presented graphically. Energy levels, transition probabilities and some other properties of atomic oxygen are summarized to aid understanding of the collision processes. The literature was surveyed through December 1988, but more recent data, if they are available to the authors, are included also.

Key words: atomic oxygen; cross section; electron collision; energy levels; oscillator strength; photoionization.

Contents

List of Tables

List of Figures

1. Introduction

Recently the present authors published compilations of cross-section data for the collision of electrons and photons with nitrogen (N_2)[1] and oxygen (O_2)[2] molecules. These molecules are the major constituents of the Earth's atmosphere. Atomic oxygen (O) is also important in the upper atmosphere of the Earth, since it is the most abundant species at heights between 200 and 600 km. Furthermore, atomic oxygen plays a significant role in the atmospheres of other planets (e.g., Venus and Mars) and in various astronomic objects. As an extension of the previous work on N_2 and O_2, the present paper compiles the cross-section data for the collision of electrons and photons with O.

The principle and detailed procedure of compilation and the evaluation of the data are essentially the same as in the previous papers.[1,2] The compilation is based on experimental data, as much as possible. In some cases, theoretic results are shown with the experimental data so that the reliability of the calculations can be seen. Where there are no experimental data available, only theoretic data are given. The collision processes considered here are only those with the atomic oxygen, in its ground state. Collisions with oxygen ions are excluded. (Cross sections for the electron impact excitation of O^{n+} were compiled by Itikawa *et al.*[3] and those for the ionization of O^{n+} were collected by Bell *et al.*[4]) No data are presented on the differential cross sections with respect to scattering angles. The energy of the incident electron or photon is, in most cases, limited to < 1 keV. The literature has been surveyed through December 1988, but some more recent data were considered when available to the present authors.

In the next section, spectroscopic and other properties of O are briefly summarized. Photoionization of O is discussed in Sec. 3. In Secs. 4–7, data on electron collisions are presented. Finally a summary and discussion of future problems are given in Sec. 8.

2. Properties of Atomic Oxygen

2.1. Energy Levels

The most reliable compilation of the energy levels of atomic oxygen was made by Moore.[5] Table 2.1 shows a number of lower states and several autoionizing states which will be referred to in the following sections. Figure 2.1. gives a partial energy-level diagram of O. Both the table and the figure include only the states with total orbital angular momentum < 3 (i.e., *S*, *P*, *D* states). In Fig. 2.1, intense dipole-allowed transitions from the ground state are indicated by vertical lines with oscillator strength. A complete Grotrian diagram of O has been given by Bashkin and Stoner.[6] Except for the ground state, only the lowest level of each multiplet is shown in Table 2.1 and Fig. 2.1. Table 2.1 contains the ionization potentials for the production of ions in specific states.

Many autoionizing states are known to exist in atomic oxygen. Some of them are included in Table 2.1 and Fig. 2.1. Dehmer *et al.*,[7] for instance, made a detailed study of the autoionizing states by a photoionization experiment, which covered the wave length range 92.0–65.0 nm.

TABLE 2.1. Energy levels of lower states of atomic oxygen. Some autoionizing states and ionization potentials are also listed

State	Configuration	Energy (eV)[a]
O^{2+} (^3P)		48.77
O^{+} ($^2P^0$)		18.64
O^{+} ($^2D^0$)		16.94
$4d'\ ^3P^0$	$2s^22p^3\ (^2D^0)4d$	16.11
$2p^5\ ^3P^0$	$2s2p^5$	15.66
$3d'\ ^3P^0$	$2s^22p^3\ (^2D^0)3d$	15.29
$3s''\ ^3P^0$	$2s^22p^3\ (^2P^0)3s$	14.12
O^{+} ($^4S^0$)		13.618
$7d\ ^3D^0$	$2s^22p^3\ (^4S^0)7d$	13.34
$6d\ ^3D^0$	$2s^22p^3\ (^4S^0)6d$	13.24
$5d\ ^3D^0$	$2s^22p^3\ (^4S^0)5d$	13.07
$4d\ ^3D^0$	$2s^22p^3\ (^4S^0)4d$	12.76
$4d\ ^5D^0$	$2s^22p^3\ (^4S^0)4d$	12.75
$3s'\ ^1D^0$	$2s^22p^3\ (^2D^0)3s$	12.73
$3s'\ ^3D^0$	$2s^22p^3\ (^2D^0)3s$	12.54
$4p\ ^3P$	$2s^22p^3\ (^4S^0)4p$	12.36
$4p\ ^5P$	$2s^22p^3\ (^4S^0)4p$	12.29
$3d\ ^3D^0$	$2s^22p^3\ (^4S^0)3d$	12.09
$3d\ ^5D^0$	$2s^22p^3\ (^4S^0)3d$	12.08
$4s\ ^3S^0$	$2s^22p^3\ (^4S^0)4s$	11.93
$4s\ ^5S^0$	$2s^22p^3\ (^4S^0)4s$	11.84
$3p\ ^3P$	$2s^22p^3\ (^4S^0)3p$	10.99
$3p\ ^5P$	$2s^22p^3\ (^4S^0)3p$	10.74
$3s\ ^3S^0$	$2s^22p^3\ (^4S^0)3s$	9.521
$3s\ ^5S^0$	$2s^22p^3\ (^4S^0)3s$	9.146
$2p^4\ ^1S$	$2s^22p^4$	4.190
$2p^4\ ^1D$	$2s^22p^4$	1.967
$2p^4\ ^3P_0$	$2s^22p^4$	0.0281
$^3P_1$	$2s^22p^4$	0.0196
$^3P_2$	$2s^22p^4$	0

[a] Except for the ground state, the energy of the lowest level of each multiplet is given. All values are taken from the NBS Table (Ref. 5).

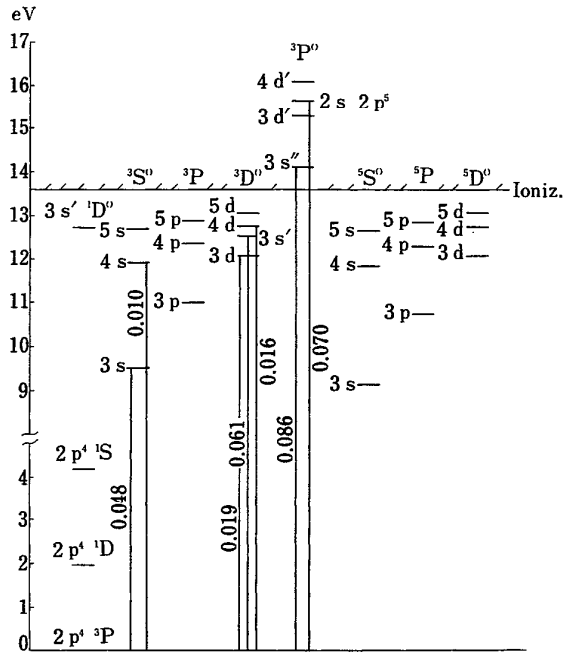

FIG. 2.1. Partial energy level diagram of atomic oxygen. Vertical lines indicate those optically allowed transitions from the ground state, which have relatively large transition probabilities. The oscillator strength measured by Doering *et al.*[9] is shown along the respective vertical line.

Atomic oxygen can capture an electron to form a negative ion (O^-). The electron affinity (EA) of atomic oxygen has been determined very precisely by the method of laser photodetachment (Neumark *et al.*[8]):

$$EA(O) = 1.461122 \pm 0.000003 \text{ eV}. \quad (2.1)$$

2.2. Oscillator Strength and Lifetime

Doering *et al.*[9] determined the absorption oscillator strength for the seven most intense dipole-allowed transitions of O. They used the electron-impact method. Table 2.2 shows the oscillator strengths they obtained. These values are also shown in Fig. 2.1. On the consideration of their accuracy, these data supercede the old NBS (now, NIST) table.[10]

In their experiment, Doering *et al.* normalized each oscillator strength to the value for the 130.4-nm transition. They had surveyed previous data on the transition and confirmed that the experimental values of the oscillator strength for the 130.4-nm transition were ~0.048 with ± 5% error. Independently of this work, Jenkins[11] measured the oscillator strength to be 0.053 ± 0.006. This is a little larger than the value adopted by Doering *et al.*, but the two values are consistent within the errors claimed.

There have been a large number of calculations of the oscillator strength of atomic oxygen. Among others, the calculation by Pradhan and Saraph[12] is the most comprehensive. Their calculation is based on the close-coupling method with the frozen core approximation. Their values are compared in Table 2.2 with the measurement of Doering *et al.* The agreement with the experimental data is quite good (within 20%). Pradhan and Saraph reported oscillator strengths for many allowed transitions other than those shown in Table 2.2.

The decay rates of the two autoionizing states, $3s''\ ^3P^0$ and $2s2p^5\ ^3P^0$, were studied in detail by Dehmer *et al.*[13] They observed both the ejected electron and the fluorescence and therefrom determined the autoionization/emission branching ratio. With the use of theoretical emission rates,[14] they finally obtained the decay rate of those states. For $2s2p^5\ ^3P^0$, the emission rate used by Dehmer *et al.* is somewhat larger than the value deduced from the oscillator strength in Table 2.2. Combining the oscillator strength in Table 2.2, with the branching ratio of Dehmer *et al.*, we get the following lifetimes:

0.79×10^{-9} s	for $3s''\ ^3P^0$	$J=0$
0.44×10^{-9} s	for	$J=1$
0.87×10^{-9} s	for	$J=2$
0.54×10^{-9} s	for $2s2p^5\ ^3P^0$	$J=0$
0.60×10^{-9} s	for	$J=1$
0.72×10^{-9} s	for	$J=2$.

The present result for $2s2p^5\ ^3P^0$ is, however, inconsistent with a beam-foil measurement [$(0.33 \pm 0.03)\times10^{-9}$ s by Knystautas *et al.*[15]]. A further study is needed to solve this discrepancy. The lifetime for $3s''\ ^3P^0$ is consistent with the beam-foil data [$(0.92 \pm 0.09)\times10^{-9}$ s by Smith *et al.*[16]].

Forbidden transitions among the states of the $2p^4$ configuration are important in various astronomical objects. Very recently Baluja and Zeippen[17] made a comprehensive calculation of the excitation energies and the probabilities for those transitions. They used a configuration interaction wavefunction and took into account a relativistic correction. Their line strengths are in agreement with the result of another detailed calculation conducted by Froese Fischer and Saha.[18] Baluja and Zeippen presented the most reliable values of the transition probabilities by combining their theoretic line strengths with the experimental excitation energies.[5] Those transition probabilities are given in Table 2.3.

In Table 2.3, some experimental results are also shown. They are all in accord with the theoretic ones, except for the $^1S_0$–$^3P_1$ (297.2 nm) transition. The experimental value for the transition was deduced from both the measured intensity ratio of the 297.2-nm line to the 557.7-nm one and the absolute value of the transition probability for the latter line. Unfortunately, the wave lengths of the two lines are widely apart so that an accurate determination of the intensity ratio is difficult.

The lifetime of the state $3s\ ^5S^0$ (for which a transition from the ground state is forbidden) was investigated by several authors. After a survey of the work, Zeippen *et al.*[19] determined the best value of the lifetime to be $(170 \pm 25)\times10^{-6}$ s.

TABLE 2.2. Oscillator strengths for the dipole allowed transitions from the ground state of O

State	Experiment: Doering *et al.*[a,b] (1985)	Experiment: Jenkins[c] (1985)	Theory: Pradhan & Saraph[d] (1977)
$2p^5\ ^3P^0$	0.070 ± 0.004[e]		0.0695
$3s''\ ^3P^0$	0.086 ± 0.006		0.0791
$4d\ ^3D^0$	0.016 ± 0.006		0.0148
$3s'\ ^3D^0$	0.061 ± 0.006		0.056
$3d\ ^3D^0$	0.019 ± 0.001		0.0203
$4s\ ^3S^0$	0.010 ± 0.002		0.00924
$3s\ ^3S^0$	0.048[b]	0.053 ± 0.006	0.0537

[a] Reference 9.
[b] All the measurements of Doering *et al.*[9] have been normalized to the value for $3s\ ^3S^0$, which is an average value of previous experimental data with ± 5% scattering.
[c] Reference 11.
[d] Reference 12.
[e] Accuracy is estimated to be within ± 5% plus the experimental deviation shown for each data.

2.3. Polarizability

Teachout and Pack[20] compiled data on the static dipole polarizability of all atoms. They determined the best value for the atomic oxygen to be

$$\alpha(\text{experiment}) = (0.77 \pm 0.06)\times10^{-24} \text{ cm}^3. \quad (2.2)$$

This is based on the measurement by Alpher and White.[21] To the knowledge of the present authors, no experimental data have been reported since 1971.

On the other hand, there are many theoretic or empirical determinations of α for O. The best calculation has been done by Werner and Meyer.[22] They used highly correlated

TABLE 2.3. Probabilities (in s^{-1}) for the transitions among the fine structure levels of $2p^4$ ^3P, ^1D, ^1S of O

State	Wave length (nm)	Recommended[a]	Experiment
$^3P_1 - {}^3P_2$	6.319×10^4	8.957×10^{-5}	
$^3P_1$		8.957×10^{-5}[b]	
		(life 1.116×10^4 s)	
$^3P_0 - {}^3P_2$	4.406×10^4	1.203×10^{-10}	
$^3P_0 - {}^3P_1$	1.455×10^5	1.735×10^{-5}	
$^3P_0$		1.735×10^{-5}[b]	
		(life 5.764×10^4 s)	
$^1D_2 - {}^3P_2$	630.0	5.627×10^{-3}	$(5.15\pm1.25)\times10^{-3}$[c]
$^1D_2 - {}^3P_1$	636.4	1.818×10^{-3}	$(1.66\pm0.42)\times10^{-3}$[c]
$^1D_2 - {}^3P_0$	639.2	8.922×10^{-7}	
$^1D_2$		7.446×10^{-3}[b]	
		(life 134.3 s)	
$^1S_0 - {}^3P_2$	295.8	2.732×10^{-4}	
$^1S_0 - {}^3P_1$	297.2	7.601×10^{-2}	$(4.5\pm1.4)\times10^{-2}$[c]
$^1S_0 - {}^1D_2$	557.7	1.215	1.06 ± 0.32[c]
$^1S_0$		1.291[b]	1.31 ± 0.05[d]
		(life 0.7744 s)	

[a] Reference 17.
[b] Decay constant in s^{-1}. The corresponding lifetime is shown in the parentheses below.
[c] Reference 81.
[d] Reference 80.

wavefunctions and produced good results for many atoms and molecules. Their value for oxygen is

$$\alpha(\text{theory}) = 0.8020\times10^{-24}\ \text{cm}^3. \quad (2.3)$$

This is consistent with the experimental value presented above.

There are two reports on the moments of the dipole oscillator strength distribution for O. Dehmer *et al.*[23] (partly revised by Inokuti *et al.*[24]) based their calculation on a simple wavefunction of Hartree–Slater type. Zeiss *et al.*[25] derived their moments empirically from photoabsorption data. The latter data are rather old and somewhat different from the more recent ones (see Sec. 3). Both sets of values for the moments of the dipole oscillator strengths, therefore, are not reliably accurate to be shown here.

3. Photoionization

Photoionization of atomic oxygen was thoroughly reviewed by Seaton.[26] A very detailed measurement of the photoionization cross section of O was made by Samson and Pareek[27] for the wavelengths 12.0–91.0 nm. They used a spark discharge lamp as the light source and detected O^+ with the use of a mass analyzer. They produced oxygen atoms with a microwave discharge of O_2. From the mesurement of the ions with the microwave discharge switched on and off, they eliminated the contribution of the dissociative ionization of O_2. Very recently Angel and Samson[28] remeasured the cross section in more detail using synchrotron radiation as the light source. They extended the wavelength region covered down to 4.43 nm. They measured cross sections also for the production of O^{2+} and O^{3+}. The result of the measurement by Angel and Samson was smoothed and plotted in Fig. 3.1.

Angel and Samson obtained the absolute value of the cross section by normalizing their relative data to the absolute measurement by Samson and Pareek. The latter authors estimated an uncertainty of their measurement to be within 9%. By using the sum rule of the oscillator strength as a

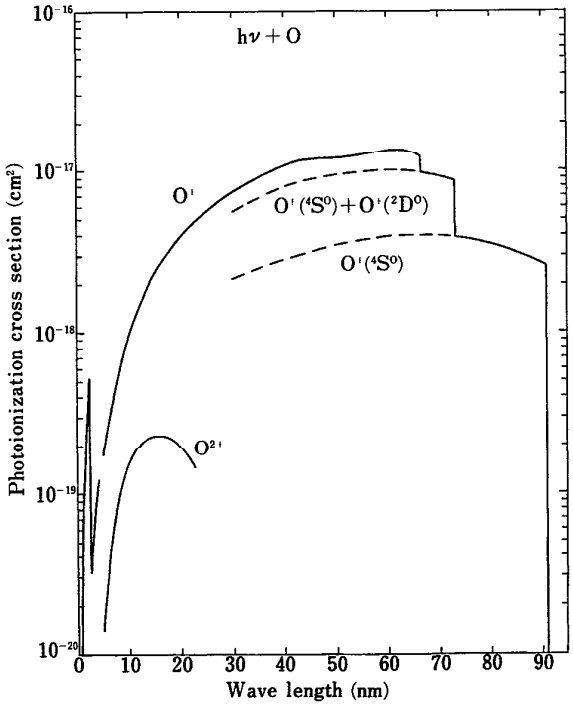

FIG. 3.1. Photoionization cross sections of O. The ions produced are indicated. The fine structure due to autoionization is smoothed out. The line below 5 nm actually shows the photoabsorption cross section, which includes multiple ionization.

constraint, Angel and Samson found that the continuum oscillator strength derived from their cross section, should be accurate to within 4.4%.

In 1979, Kirby *et al.*[29] determined the best value of the photoionization cross section on the basis of the data then available. For wavelengths >30.0 nm, there is an overall agreement between their data and the present ones. The former values are somewhat larger than the latter in the shorter wavelength region.

The dashed lines in Fig. 3.1 show the partial cross sections for the production of O^+ (^4S) and O^+ (^4S) + O^+ (^2D). These lines are drawn in the same way as Angel and Samson, i.e., by an extrapolation of the cross section, measured near threshold, through the partial cross sections, determined by the branching ratios measured at 58.4 (by Samson and Petrosky[30]) and 30.4 nm (by Dehmer and Dehmer[31]). Hussein *et al.*[32] measured the branching ratio over the wavelengths 58.0–72.5 nm. They also used synchrotron radiation. The present partial cross sections are generally consistent with those deduced from the branching ratio obtained by Hussein *et al.*

There are a large number of calculations of photoionization cross section of O (see, for instance, the review by Seaton[26]). Angel and Samson[28] made a detailed comparison of their measurement to more than ten sets of calculations. They found that most of the theoretic data lie within 40% of the experimental ones. The details of the agreement, however, are very different depending on the method of calculation and the wavelength range considered.

At wavelengths >40.0 nm, autoionization has a large effect. Because of the complicated structure, any contribution of autoionization is not shown in Fig. 3.1. Below the ^2P threshold (66.5 nm), Dehmer *et al.*[7] measured a very detailed autoionization spectrum. Angel and Samson[28] reported autoionizing resonance leading to the ^4P threshold (43.5 nm). A theoretical study of autoionization was carried out by several authors (e.g., Pradhan[33]). Seaton[26] made a detailed discussion of the work in his review.

For wavelengths <5 nm, we plot in Fig. 3.1 the photoabsorption cross section recommended by Henke *et al.*[34] This cross section includes the contribution of multiple ionization. The K edge (i.e., the threshold of the ejection of the $1s$ electron) of oxygen is located at 2.332 nm.

Angel and Samson[28] measured also, the cross sections for the production of O^{2+} and O^{3+} in the region 4.4–25.4 nm. The cross section for the double ionization is plotted in Fig. 3.1. The triple ionization is very rare in the region considered (the maximum cross section being 2.20×10^{-21} cm^2 at 8.27 nm). Multiple ionization probably plays a significant role in the higher energy region above the K edge.

4. Electron Collisions: Total-Scattering, Elastic and Momentum-Transfer Cross Sections

4.1. Elastic and Momentum-Transfer Cross Sections

There is only one measurement of the elastic cross section, Q_{elas}, reported so far for atomic oxygen. Dehmel *et al.*[35] measured differential cross sections (DCS) for the elastic scattering at 5 and 15 eV of electron energy. (Actually their DCS includes the contribution of inelastic scattering, but they estimated the latter contribution to be $<25\%$.) They normalized their data in relative magnitude to the total scattering cross section (Q_T) of Sunshine *et al.*[36] The absolute magnitude of the data reported by Dehmel *et al.*, therefore, provides no new information, but the angular distribution of the cross section can be used to test any theoretic result.

On the other hand there are a large number of theoretic calculations of Q_{elas}, for atomic oxygen. In the lower energy region (<10 eV), induced polarization plays an essential role in the scattering of electrons on atoms. Calculations with the polarization effect included, were made by Vo Ky Lan *et al.*,[37] Rountree *et al.*,[38] Thomas and Nesbet,[39,40] and Tambe and Henry.[41,42] The DCS calculated by Tambe and Henry[42] shows good agreement with those measured by Dehmel *et al.* Their calculation includes an adequate short-range correlation between the incident and the target electrons. The Q_{elas} obtained by Tambe and Henry[41] is shown in Fig. 4.1.

In the higher energy region (>10 eV), most of the calculations rely on simple models. The most elaborate one is the calculation by Blaha and Davis.[43] They used a distorted wave method, thus taking into account the distortion of the scattered electrons, by the target. They approximately include, in their calculation, the effects of polarization and electron exchange. Blaha and Davis reported Q_{elas} for the

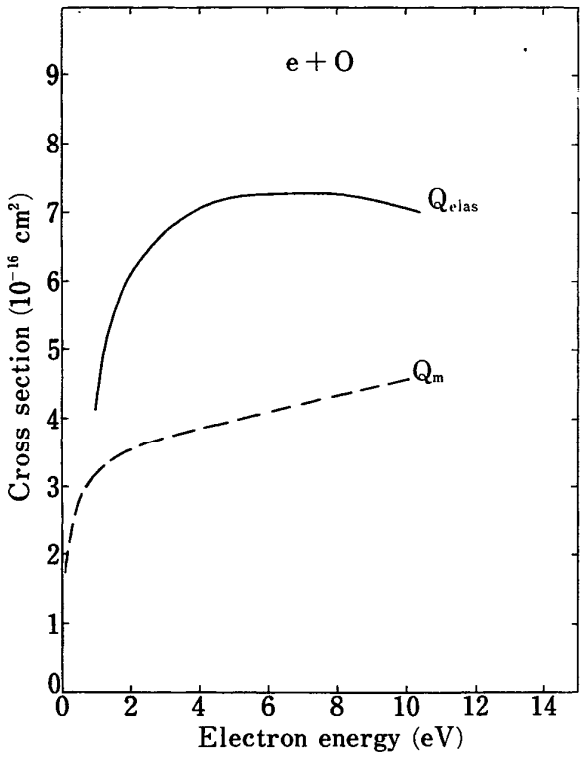

FIG. 4.1. Elastic (Q_{elas}) and momentum-transfer (Q_m) cross sections for electron collisions with O.

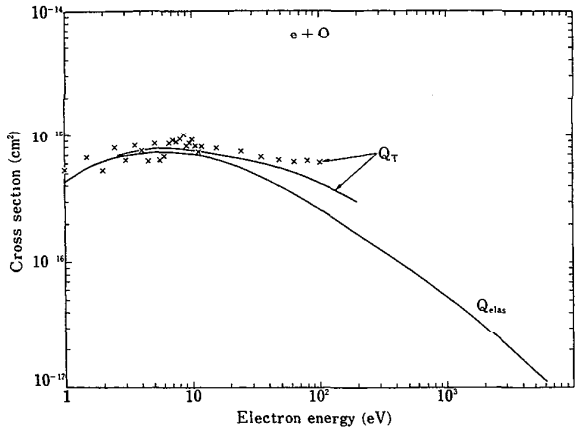

FIG. 4.2. Elastic (Q_{elas}) and total-scattering (Q_T) cross sections for electron collisions with O. Crosses are the Q_T measured by Sunshine *et al.*[36]

energies 1–500 eV, but their method is less reliable at lower energies. In the present paper, we connected the Q_{elas} of Blaha and Davis for $E_e > 50$ eV to the Q_{elas} of Tambe and Henry for $E_e < 10$ eV to produce the "best" cross section. The result is given in Fig. 4.2. In Fig. 4.2, the cross-section curve is extended to the region $E_e > 500$ eV, on the consideration of the calculation by Riley *et al.*[44] for $E_e \geqslant 1$ keV. Riley *et al.* solved a scattering equation with the electrostatic potential of O.

Only the paper by Thomas and Nesbet[40] reported momentum–transfer cross section Q_m for atomic oxygen. Their Q_m is shown in Fig. 4.1. The DCS of Thomas and Nesbet is somewhat different from that of Tambe and Henry (see Ref. 42), which has been chosen as the best value of Q_{elas} (Fig. 4.1). It is uncertain how the difference in the DCS affects the resulting Q_m.

4.2. Total Scattering Cross Section

Sunshine *et al.*[36] reported their measurement of the total scattering cross section Q_T for atomic oxygen. Due to the difficulty of the experiment, their data scatter rather widely. Here we estimate Q_T with the formula,

$$Q_T = Q_{elas} + \sum Q_{exc}(n) + \sum Q_{ion}(O^{q+}), \qquad (4.1)$$

where the three terms in the right hand side of Eq. (4.1) indicate the cross sections for elastic scattering, excitation of the electronic state n, and productin of the ion O^{q+}, respectively. Numerical values of Q_{elas} and Q_{ion} are taken from Figs. 4.2 and 6.1, respectively. We take into account all the excitation processes mentioned in Sec. 5 (most of the Q_{exc} considered here being shown in Fig. 8.1). The resulting Q_T is given in Fig. 4.2 to compare with the data of Sunshine *et al.*

The Q_T obtained here is generally consistent with the experimental value. In the energy region higher than 50 eV, some discrepancy exists between the two results. A part of the difference may be ascribed to the excitation processes for which no data are available at present, but the difference at 100 eV ($\sim 2\times 10^{-16}$ cm^2) is too large to be reconciled with such missing excitation processes alone. We need a more elaborate experimental determination of Q_T.

5. Electron Collisions: Electronic Excitations

5.1. Fine Structure Transition in the Ground State

The ground state of O has a fine-structure (FS) splitting as shown in Table 2.1. The transition among the FS levels (^3P_J with $J = 2,1,0$) leads to an important cooling mechanism of the electron gas in the Earth's ionosphere and a variety of astrophysical plasmas. Carlson and Mantas[45] reviewed the four sets of cross sections then available for the FS transition: Breig and Lin,[46] Saraph,[47] Tambe and Henry,[41,48] and LeDourneuf and Nesbet.[49] Very recently Berrington[50] reported his elaborate calculation of the FS transition. He applied the R-matrix method to the calculation while including $2p^4$ ^3P, ^1D, ^1S terms and some pseudostates. He presented only the collision strength in his paper. Figure 5.1 shows the cross sections for the FS excitations, $J = 2 \rightarrow 1$, $2 \rightarrow 0$, and $1 \rightarrow 0$, deduced from the collision strengths of Berrington. He compared his result to the previous calculations mentioned above. A large disagreement was found in the lower energy region, while a reasonable agreement is seen at higher energies.

A quantity of practical importance is the cooling rate defined in the form

$$\left\langle \frac{dE}{dt} \right\rangle = n_e n_o \sum_J f_J(T_g) \sum_{J'} \Delta E(J \rightarrow J') k(J \rightarrow J' | T_e). \quad (5.1)$$

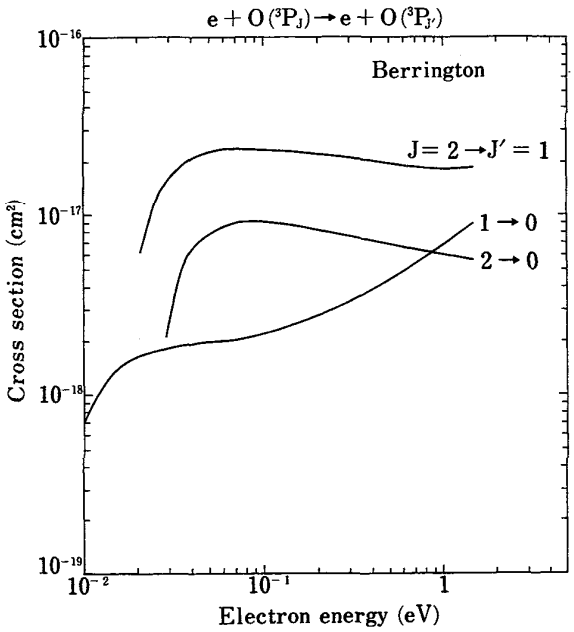

FIG. 5.1. Cross sections for the transition of fine-structure levels ($^3P_J \rightarrow {}^3P_{J'}$) of atomic oxygen, calculated by Berrington.[50]

TABLE 5.1. Rate coefficient ($\langle dE/dt \rangle/(n_o n_e)$ in 10^{-11} eV cm^3 s^{-1}) of the cooling of electron gas due to the fine structure transitions in the ground state of O

	T_g (K)[b]			
T_e (K)[a]	100	300	1000	3000
200	0.203			
500	0.676	0.181		
1000	1.08	0.436		
2000	1.51	0.690	0.136	
5000	2.62	1.27	0.359	0.061
10000	4.32	2.13	0.655	0.173

[a] Electron temperature in K.
[b] Temperature of the oxygen gas in K.

Here n_e and n_o are the number densities of electron and oxygen atom, respectively, $f_J(T_g)$ is the fractional population of each FS level of O (depending on the temperature T_g of the oxygen gas), $\Delta E(J \rightarrow J')$ is the energy loss (gain) due to the excitation (deexcitation) $J \rightarrow J'$, and $k(J \rightarrow J'|T_e)$ is the rate coefficient for the process $J \rightarrow J'$ at the electron temperature T_e. Berrington reported in his paper the effective collision strength (i.e., the collision strength integrated over a Maxwellian distribution of electron velocities). Using this effective collision strength, we can easily calculate the rate coefficient $k(J \rightarrow J')$ and therefrom $\langle dE/dt \rangle$. The result is shown in Table 5.1.

When compared to the cooling rate based on the calculation of Tambe and Henry[41] (given in Ref. 45), the present value is somewhat larger than theirs. From the observation of the ionospheric temperature, Carlson and Mantas[45] suggested that the cooling rate of Tambe and Henry is too large. It is urgently required, therefore, that the theoretic cross section be tested directly by experiment.

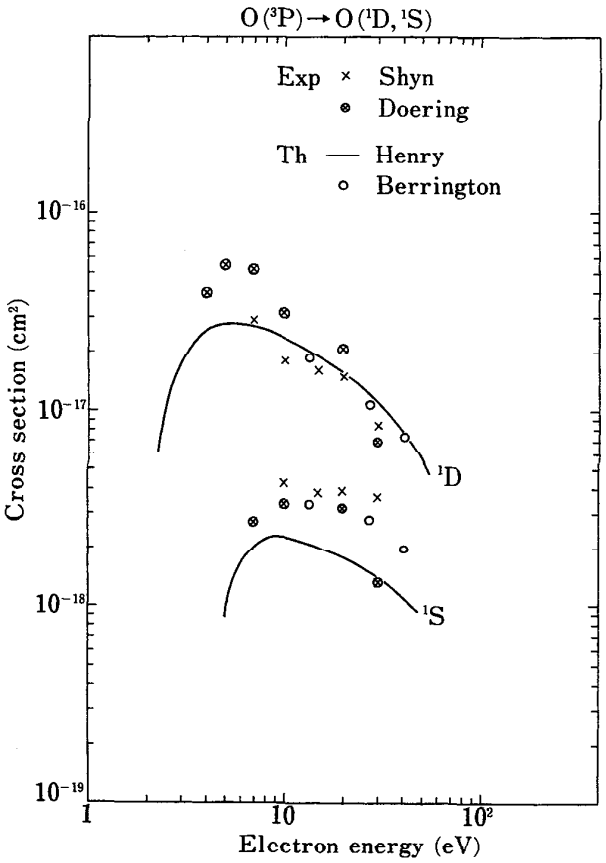

FIG. 5.2. Cross sections for excitations of $2p^4$ ^1D and ^1S states. Experimental values obtained by Shyn and Sharp,[52] Shyn *et al.*,[53] and Doering and Gulcicek[54] are compared with theoretical ones by Henry *et al.*[56] and Berrington (Ref. 55 and private communication).

5.2. Excitations of $2p^4$ ^1D, ^1S States

Until recently no measurement of the cross section for the excitation of $2p^4$ ^1D and ^1S states has been reported, though several different sets of theoretic calculations have been available. In 1985, Shyn and Sharp[51] reported for the first time the experimental cross section for the excitation of the ^1D state. The measurement was made only at 20 eV of electron energy. Later they published a wider range of experiment[52] and extended their measurement to the excitation of $2p^4$ ^1S state.[53] Very recently Doering and Gulcicek[54] made quite a similar measurement of Q_{exc} ($2p^4$ ^1D) and Q_{exc} ($2p^4$ ^1S). The two sets of the experimental data are shown in Fig. 5.2.

There seems to be some difference between the results of the two experiments. If we consider rather large uncertainties of those data, however, the two experimental results are consistent with each other. (Shyn *et al.*[52,53] claimed the error to be 50% for ^1D and 54% for ^1S, while Doering and Gulcicek[54] estimated the corresponding uncertainties to be 35% and 40%.) Both groups deduced the cross section from their measurement of electron energy loss spectra (ELS) for a mixture of O and O_2. Doering and Gulcicek obtained a large fraction (25%–50%) of atomic oxygen using a microwave discharge. Shyn *et al.* achieved 7% O with an oven. Furthermore, Doering and Gulcicek used an electron energy analyzer with a higher resolution (80–120 meV) than Shyn *et al.* (150 meV). Thus the ELS obtained by the former authors are much sharper than those by the latter. These and other differences in the experimental conditions would make the cross section obtained by Doering and Gulcicek more reliable.

The most recent and elaborate calculation of the cross sections Q_{exc} ($2p^4$ ^1D) and Q_{exc} ($2p^4$ ^1S) is the work done by Berrington (private communication; only rate coefficients being published by Berrington and Burke[55]). He made an R-matrix method calculation with including eight target states. In Fig. 5.2, the theoretic values are plotted at three points of energy. The theoretic cross sections of Henry *et al.*[56] are also presented in the figure, as a typical example of previous calculations. Berrington's cross sections are in fairly good agreement with the experimental data.

5.3. Excitations of Other States

From their measurement of electron energy loss, Doering and his colleagues at the Johns Hopkins University obtained excitation cross sections for a number of states of the

oxygen atom. These cross sections are shown here together with some results of theoretic calculations. There are two sets of comprehensive calculations available. Smith[57] made a close-coupling calculation for a number of excitation processes. Recently Tayal and Henry carried out a calculation based on the R-matrix method. They reported cross sections first for the $3s\ ^3S^0$ and $3p\ ^3P$ excitations.[58] Then they extended their calculation to the excitations of $3s\ ^5S^0$, $3p\ ^5P$, $3d\ ^3D^0$, $3s'\ ^3D^0$, $4s\ ^3S^0$, and $4p\ ^3P$ states.[59] Tayal and Henry used many more coupled states in their calculation. Thus the cross section obtained by Tayal and Henry should, in principle, be more accurate than that of Smith. As is shown later, however, the agreement with experiment is not always better for the former result than for the latter. This indicates that it is very difficult to do a reliable calculation for the excitation of O.

For convenience, Table 5.2 lists the electronic states for which an excitation cross section is given in the present paper. A comparison with the emission cross section, if any, is made in the next subsection.

5.3.a. $3s\ ^3S^0$ and $4s\ ^3S^0$

Figure 5.3 shows the experimental cross section for the $3s\ ^3S^0$ excitation. The data for energies higher than 30 eV are taken from the paper by Vaughan and Doering.[60] They smoothed the original data of differential cross section[61] by fitting to an analytical form and evaluated Q_{exc} with them. Below 30 eV, the values revised by Gulcicek and Doering[62] are plotted in Fig. 5.3.

The calculations by Smith[57] and by Tayal and Henry[58] are also shown in Fig. 5.3. Here the two-state close-coupling calculation of Smith at higher energies (>20 eV) is combined with his five-state one near the threshold. (Smith made the five-state calculation only near the threshold). Tayal and Henry employed the R-matrix method including

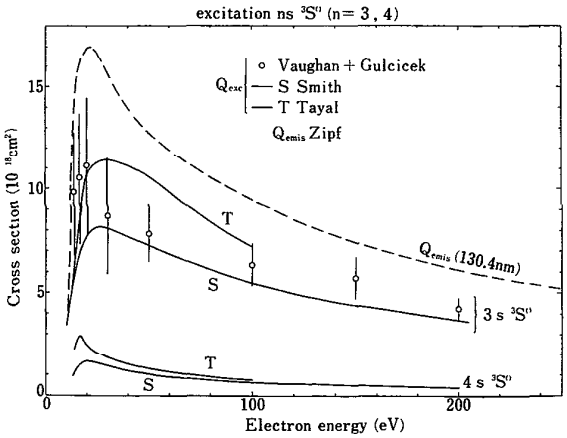

FIG. 5.3. Cross sections for excitations of $3s\ ^3S^0$ and $4s\ ^3S^0$ states of O. For the $3s\ ^3S^0$ excitation, two sets of theoretic data (S: Smith[57] and T: Tayal and Henry[58]) are compared with experiment (open circles: Vaughan and Doering[60] with the revision of Gulcicek and Doering[62] in the region <30 eV). For comparison, emission cross section for the 130.4-nm line ($3s\ ^3S^0 \rightarrow 2p^4\ ^3P$)[68] is also shown (dashed line). For $4s\ ^3S^0$, only the theoretical values[57,59] are plotted.

up to 12 states of oxygen. Smith's cross section shows an overall agreement with the experimental result except in the region below 20 eV, where the cross section of Tayal and Henry seems very reasonable.

There is no measurement of the cross section for the excitation of the $4s\ ^3S^0$ state. In Fig. 5.3, we give the results of the two-state close-coupling calculation by Smith[57] and the R-matrix method calculation by Tayal and Henry.[59] Except in the low-energy region (<30 eV), the two sets of calculations are in reasonable agreement. Vaughan and Doering[63] give, in their paper, an electron ELS at the incident energy of 100 eV. The spectrum clearly shows the energy-loss peak due to the excitation of the $4s\ ^3S^0$ state. The ratio of the peak heights of the $3s\ ^3S^0$ excitation to the $4s\ ^3S^0$ one is ~ 10. This value almost coincides with the ratio of Smith's cross sections at 100 eV, thus confirming the reliability of the theoretic result for the $4s\ ^3S^0$ excitation near 100 eV.

5.3.b. $3p\ ^3P$ and $4p\ ^3P$

Gulcicek *et al.*[64] measured the cross section for the excitation of the $3p\ ^3P$ state. Their values are shown in Fig. 5.4.

Tayal and Henry[58] reported the corresponding theoretic values, which are also shown in Fig. 5.4. Except near threshold, the discrepancy of theory from experiment is very large. There are two other calculations: Smith[57] using a two-state close-coupling method and Sawada and Ganas[65] using a distorted wave approximation. Both the calculations give also too large a cross section compared to the experimental value.

Tayal and Henry[59] gave the cross section for the excitation of the $4p\ ^3P$ state. Their cross section is also shown in Fig. 5.4. In this case, there is no experimental data for comparison.

TABLE 5.2. Excited states of atomic oxygen for which excitation (Q_{exc}) and emission (Q_{emis}) cross sections are given in the present paper. The original data sources are shown for each cross section

State	Reference Q_{exc}	Reference Q_{emis}	Figure
$4d'\ ^3P^0$	63(E)[a]		5.8
$2p^5\ ^3P^0$	63(E)		5.8
$3s''\ ^3P^0$	63(E)	69	5.8
$7d\ ^3D^0$	63(E)		5.6
$6d\ ^3D^0$	63(E)		5.6
$5d\ ^3D^0$	63(E)		5.6
$4d\ ^3D^0$	63(E)		5.6
$3s'\ ^3D^0$	60,62(E) 59(T)	68	5.7
$4p\ ^3P$	59(T)		5.4
$3d\ ^3D^0$	63(E) 57,59(T)	68	5.5,5.6
$4s\ ^3S^0$	57,59(T)		5.3
$3p\ ^3P$	64(E) 58(T)		5.4
$3p\ ^5P$	64(E) 59(T)	71	5.10
$3s\ ^3S^0$	60,62(E) 57,58(T)	68	5.3
$3s\ ^5S^0$	66(E) 57,59(T)		5.9
$2p^4\ ^1S$	53,54(E) 55,56(T)		5.2
$2p^4\ ^1D$	52,54(E) 55,56(T)		5.2

[a] E: experiment; T: theory

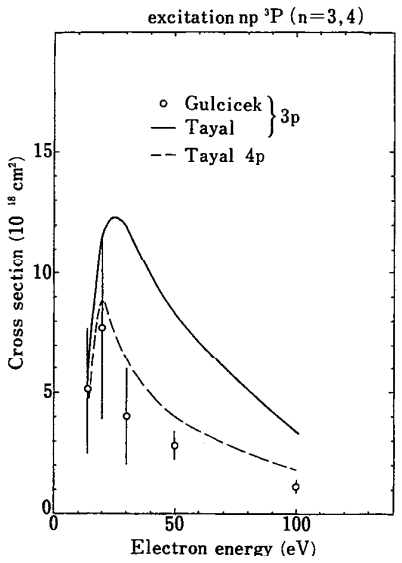

FIG. 5.4. Cross sections for excitations of $3p\,^3P$ and $4p\,^3P$ states of O. Experiment (open circles: Gulcicek *et al.*[64]) is compared with theory (solid line: Tayal and Henry[58]) for $3p\,^3P$. Only theoretical values (dashed line: Tayal and Henry[59]) are shown for $4p\,^3P$.

5.3.c. $nd\,^3D^0$ (n=3–7)

Vaughan and Doering[63] reported their measurement of the cross sections for the excitation of the $nd\ ^3D^0$ states ($n = 3,4,5,6,7$).

Figure 5.5 compares the experimental cross section for the $3d\ ^3D^0$ state to the theoretic ones obtained by Smith[57] and Tayal and Henry.[59] From the comparison, however, it is difficult to say which calculation is better.

In Fig. 5.6, the experimental cross sections for the excitation of $nd\ ^3D^0$ ($n = 4,5,6,7$) are shown together with the theoretic (Smith's) and the experimental cross sections for the $3d\ ^3D^0$ excitation (shown in Fig. 5.5). The energy dependences of the cross sections for the nd excitation look

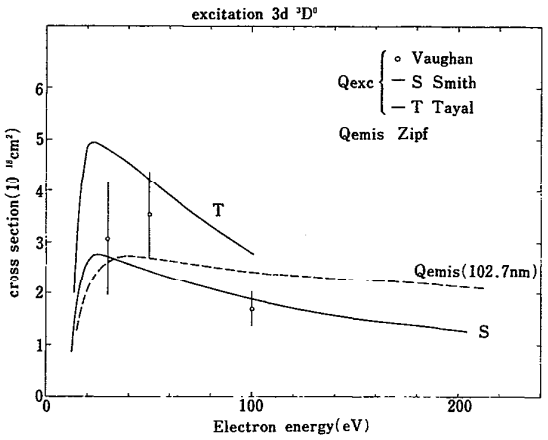

FIG. 5.5. Cross sections for excitation of $3d\,^3D^0$ state of O. Experimental values (open circles: Vaughan and Doering[63]) are compared with theoretical ones (S: Smith[57] and T: Tayal and Henry[59]). For comparison, emission cross section (dashed line) obtained by Zipf and Erdman[68] is plotted for the line 102.7 nm ($3d\,^3D^0 \rightarrow 2p^4\,^3P$).

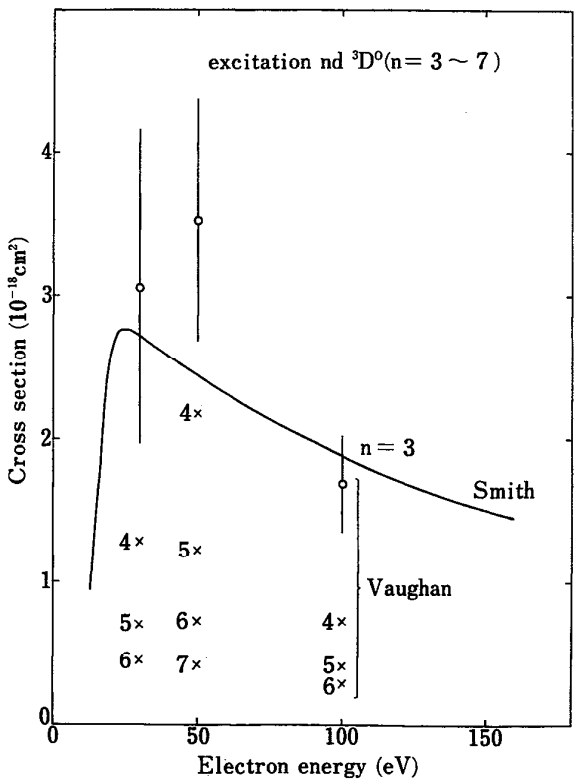

FIG. 5.6. Cross sections for excitation of $nd\ ^3D^0$(n = 3,4,5,6,7) states of O, measured by Vaughan and Doering.[63] For $3d\,^3D^0$ theoretical data (obtained by Smith[57]) are also shown.

similar to each other, as can be expected for members of the same Rydberg series.

5.3.d. $3s'\ ^3D^0$

Figure 5.7 shows a comparison of the experimental[60,62] and the theoretic[59] cross sections for the excitation of the

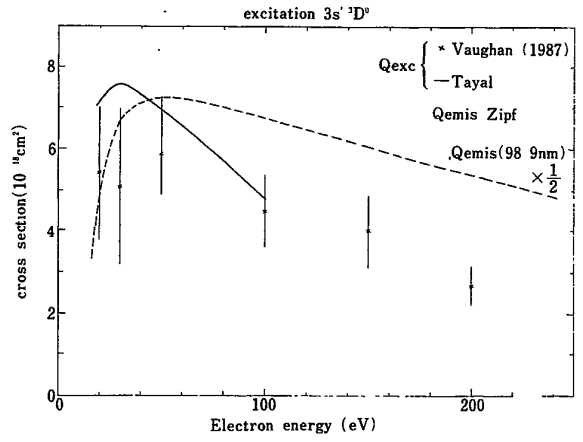

FIG. 5.7. Cross sections for excitation of $3s'\,^3D^0$ state of O. Experimental values (crosses: Vaughan and Doering[60] with a revision by Gulcicek and Doering[62] at 20 eV) are compared to theoretical ones (solid line: Tayal and Henry[59]). For comparison, emission cross section (dashed line) obtained by Zipf and Erdman[68] is plotted for the line 98.9 nm ($3s'\,^3D^0 \rightarrow 2p^4\,^3P$). Note that Q_{emis} (98.9 nm) is reduced by half to fit in the figure.

$3s'\ ^3D^0$ state. At 20 eV, Gulcicek and Doering[62] revised the cross section previously measured by Vaughan and Doering[60] because of the remeasurement of the Q_{exc} ($3s\ ^3S^0$) to which the data are normalized. The theoretic result is not inconsistent with experiment, provided that a large uncertainty of the latter is taken into account.

5.3.e. Autoionizing States ($3s''\ ^3P^0$, $2s2p^5\ ^3P^0$, $4d'\ ^3P^0$)

Vaughan and Doering[63] obtained the energy-loss spectrum corresponding to the excitation of the $3s''\ ^3P^0$, $2s2p^5\ ^3P^0$, $4d'\ ^3P^0$ states. From this spectrum, they derived the excitation cross sections shown in Fig. 5.8. Very interestingly the excitation cross section for the $3s''\ ^3P^0$ state is very close to that for the $2s2p^5\ ^3P^0$ state. Furthermore, the two cross sections have quite a large absolute magnitude. In fact, they have the largest value among the cross sections for the excitation of electronic state of O except for $2p^4\ ^1D$. There are no theoretic cross sections for comparison.

5.3.f. $3s\ ^5S^0$

Doering and Gulcicek[66] measured the cross section for the excitation of the $3s\ ^5S^0$ state. Their cross section is given in Fig. 5.9 with the two sets of theoretic ones.[57,59] Both the calculations show a rather good agreement with experiment. Near the threshold (<13 eV), Rountree[67] made another calculation and showed a sharp resonance just above the threshold. Because the experiment was done only at energies above 13.9 eV, it is still uncertain whether the resonance is real or not.

5.3.g. $3p\ ^5P$

Gulcicek *et al.*[64] measured the cross section for the excitation of the $3p\ ^5P$ state. In Fig. 5.10, the experimental cross section is compared to the theoretic value obtained by Tayal and Henry.[59] The agreement between theory and experiment is fairly good, though the theoretic peak at 16.5 eV is not confirmed experimentally.

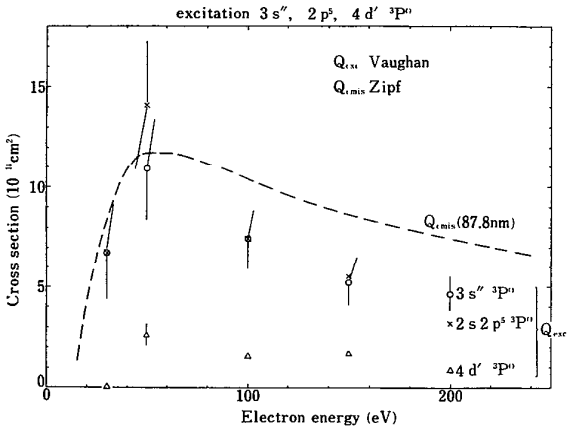

FIG. 5.8. Cross sections for excitation of the autoionizing states, $3s''\ ^3P^0$, $2s2p^5\ ^3P^0$ and $4d'\ ^3P^0$ states of O, measured by Vaughan and Doering.[63] For comparison, emission cross section (dashed line) for the 87.8-nm line ($3s''\ ^3P^0 \rightarrow 2p^4\ ^3P$) obtained by Zipf and Kao[69] is also plotted.

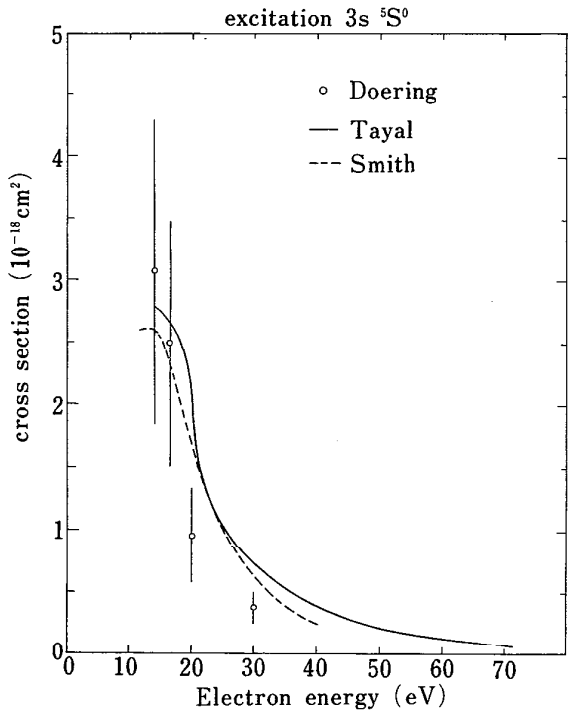

FIG. 5.9. Cross sections for excitation of $3s\ ^5S^0$. Experimental result (open circles) obtained by Doering and Gulcicek[66] is compared with two sets of calculations (solid line: Tayal and Henry[59] and dashed line: Smith[57]).

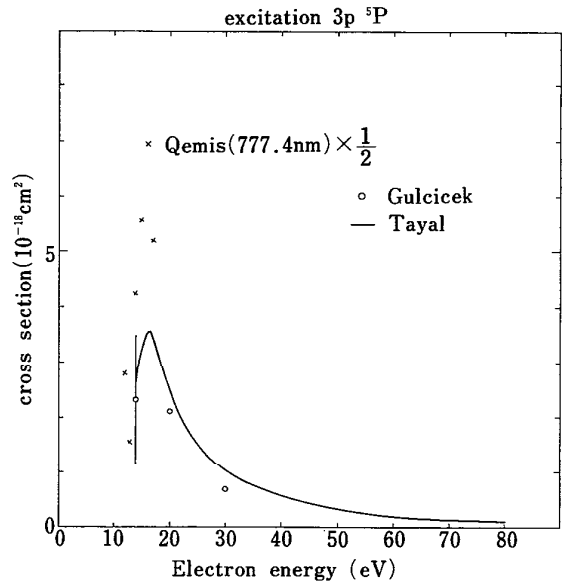

FIG. 5.10. Cross sections for excitation of $3p\ ^5P$ state of O. Experimental data (open circles) obtained by Gulcicek *et al.*[64] are compared to the calculation (solid line) by Tayal and Henry.[59] Emission cross section for the 777.4-nm line ($3p\ ^5P \rightarrow 3s\ ^5S^0$)[71] is also plotted for comparison (crosses). Note that the emission cross section is reduced by half to fit in the figure.

5.4. Emission Cross Sections

Zipf and Erdman[68] reported their experimental results of the emission cross sections for the lines 130.4 nm ($3s\,^3S^0 - 2p^4\,^3P$), 102.7 nm ($3d\,^3D^0 - 2p^4\,^3P$) and 98.9 nm ($3s'\,^3D^0 - 2p^4\,^3P$). Zipf and Kao[69] measured the Q_{emis} for another line (87.8 nm for $3s''\,^3P^0 - 2p^4\,^3P$). These four cross sections are shown together in Fig. 5.11.

The Q_{emis} for 130.4 nm was originally measured by Stone and Zipf.[70] To obtain an absolute value of the cross section, they used the cross section ratio, Q_{emis} (130.4 nm)/Q_{emis} (130.4 nm, O_2) and the absolute value of Q_{emis} (130.4 nm, O_2). Here Q_{emis} (130.4 nm, O_2) is the cross section for the emission of the 130.4-nm line due to the dissociative excitation of oxygen molecules. Both the cross-section ratio and the Q_{emis} (130.4 nm, O_2) have been recently revised. Zipf and Erdman renormalized the emission function of Stone and Zipf using these revised quantities. The values shown in Fig. 5.11 are the revised ones. The other emission cross sections shown in the figure have been obtained in a similar manner.

Now we compare the Q_{emis} to the Q_{exc} presented in the previous subsection. It should be noted that Q_{emis} includes a cascade contribution. The two cross sections, therefore, do not necessarily coincide.

In Fig. 5.3, the Q_{emis} (130.4 nm) is compared to the Q_{exc} ($3s\,^3S^0$). The difference between the two cross sections can be explained in terms of cascade. For instance, the difference around the maximum (at ~25 eV) is probably ascribed to the excitation of the $3p\,^3P$ state followed by the transition $3p\,^3P$–$3s\,^3S^0$.

In Fig. 5.5, the Q_{emis} (102.7 nm) is compared to the Q_{exc} ($3d\,^3D^0$). The Q_{emis} (102.7 nm) is in agreement with the Q_{exc} ($3d\,^3D^0$) in the enegy region $E_e < 50$ eV, but, in the higher energy region, it decreases with energy more slowly than the Q_{exc}. The latter deviation may arise from a cascade.

A comparison between Q_{emis} (98.9 nm) and Q_{exc} ($3s'\,^3D^0$) is made in Fig. 5.7. Here the former cross section has been reduced by a factor of two to enable the comparison. The Q_{emis} (98.9 nm) decreases more slowly than the Q_{exec} ($3s'\,^3D^0$). This may be due to cascade. The difference (by a factor of two) in the absolute magnitude of the two cross sections, however, is too large to be explained by cascade alone.

In Fig. 5.8, the Q_{emis} (87.8 nm) is compared to the Q_{exc} ($3s''\,^3P^0$). The state $3s''\,^3P^0$ decays either by emission of radiation (87.8 nm) or by autoionization. The autoionization/emission branching ratio was determined by Dehmer *et al.*[13] to be 1.07 (after averaging over multiplet). Thus, $2.07 \times Q_{emis}$ (87.8 nm) should coincide with the Q_{exc} ($3s''\,^3P^0$), if no cascade is involved in the emission of 87.8-nm line. When we multiply the Q_{emis} (87.8 nm) in Fig. 5.8 by 2.07, the resulting value becomes larger by a factor of 2 to 3 than the Q_{exc} ($3s''\,^3P^0$). Since the $3s''\,^3P^0$ state is located above the ionization threshold, it is very unlikely for any cascade to contribute significantly to this emission. A further study is thus needed.

Recently Germany *et al.*[71] measured the cross section for the emission of 777.4-nm radiation from the transition $3p\,^5P$–$3s\,^5S^0$. They produced atomic oxygen by photodissociating O_2 with a laser light. To avoid the contamination with the emission from the dissociative excitation of O_2, they made the measurement only below 17 eV of electron energy. The resulting emission cross section is compared in Fig. 5.10 to the Q_{exc} ($3p\,^5P$). The emission cross section has been reduced by half to be plotted in the figure. The large difference in the absolute magnitudes of the two cross sections is ascribed to a contribution of the cascade from the $ns\,^5S^0$ and $nd\,^5D^0$ levels located above the $3p\,^5P$ state.[71]

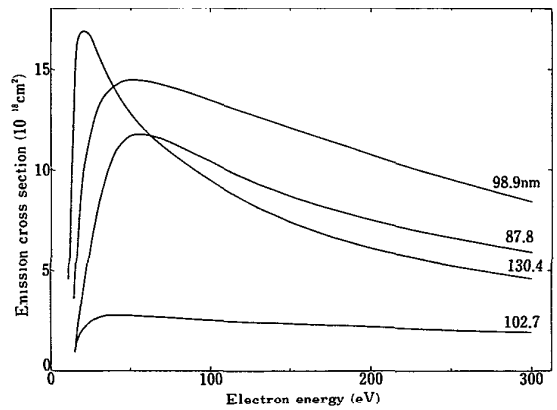

FIG. 5.11. Cross sections for emission of the lines 87.8, 98.9, 102.7 and 130.4 nm upon electron collision with O. Those cross sections were measured by Zipf and his collaborators.[68,69]

6. Electron Collisions: Ionization

Bell *et al.*[4] compiled and assessed cross-section data on the electron-impact ionization of atoms and atomic ions with $Z \leqslant 8$ (Z being the nuclear charge). For each species, they determined recommended cross sections, which were fitted by an analytical formula for practical use. For the ionization of atomic oxygen, they gave the formula

$$Q_{ion}(O^+)(\text{in } 10^{-13}\text{ cm}^2) = \frac{1}{IE_e}\left\{2.4554 \ln\frac{E_e}{I} - 2.1811\left(1-\frac{I}{E_e}\right) - 1.5701\left(1-\frac{I}{E_e}\right)^2\right\}, \quad (6.1)$$

where I is the ionization potential of the oxygen ($I = 13.62$ eV) and E_e is the electron energy in eV. Figure 6.1 shows the cross section calculated with the above formula. The cross section is based largely on the measurement by Brook *et al.*[72]

The original cross section obtained by Brook *et al.* includes, in principle, a contribution from autoionization, if any. In reality, however, the cross section shows no discernible evidence of autoionization. We can estimate the contribution caused, for instance, by the excitation of $2s2p^5\,^3P^0$ as follows: Combining the excitation cross section of the $2s2p^5\,^3P^0$ state in Fig. 5.8 with the autoionization/emission branching ratio determined by Dehmer *et al.*[13] we have the

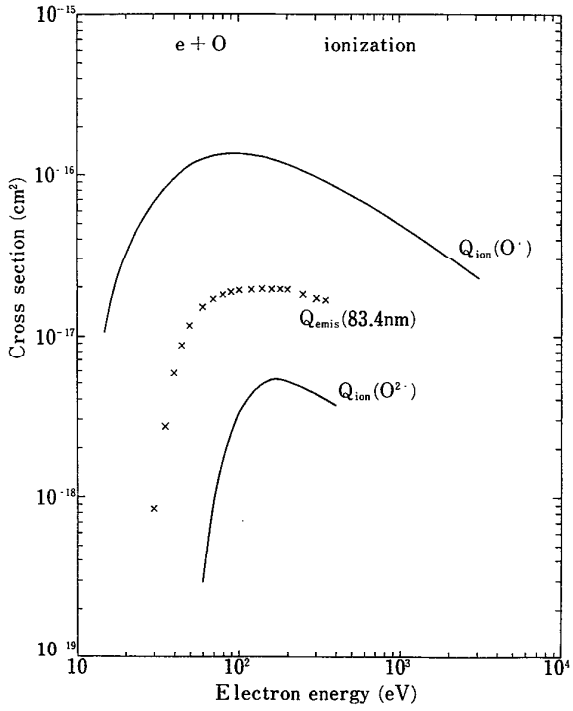

FIG. 6.1. Ionization cross sections of O for the productions of O^+ and O^{2+}. Also shown are the cross sections for the emission of 83.4 nm line ($2s2p^4\,{}^4P \rightarrow 2s^22p^3\,{}^4S^0$) of O^+, upon electron collision with O.[76]

autoionization contribution to be 0.730×10^{-17} cm^2 at 50 eV and 0.387×10^{-17} cm^2 at 100 eV. On the consideration of the accuracy of the branching ratio and the excitation cross sectin used, these values have an uncertainty of ~30%. At the lower energy, the autoionization contributes rather considerably to the ionization of oxygen.

There is no experimental information concerning the state of the ion produced. Burnett and Rountree[73] calculated the partial cross section for the production of $O^+(^4S)$, $O^+(^2P)$ and $O^+(^2D)$. According to their calculation, the fractions of $O^+(^4S)$ and $O^+(^2D)$ are almost the same, while $O^+(^2P)$ is produced by ~50% less than $O^+(^4S)$ or $O^+(^2D)$. In this calculation, only the $2p$ electron is assumed to ionize. Burnett and Rountree showed, however, that the direct ionization of the $2s$ electron is much less frequent than the $2p$ ionization. It should be noted that the calculation does not take into account autoionization. The autoionization through the excitation of the $2s2p^5\,{}^3P^0$ state, for instance, enhances the fraction of $O^+(^4S)$.

Two experimental groups[74,75] reported the ionization cross section for the production of O^{2+}. Both the groups actually measured the ratio of the ion yield, O^{2+}/O^+. They then multiplied the ratio by $Q_{ion}(O^+)$ measured by themselves (Zipf) or by other authors (Ziegler *et al.*). The ratios measured by the two groups are in close agreement with each other. Here we multiply their ratio by $Q_{ion}(O^+)$ recommended by Bell *et al.* (see Fig. 6.1). The resulting value of $Q_{ion}(O^{2+})$ is shown in Fig. 6.1.

Zipf *et al.*[76] measured the emission of 83.4-nm line ($2s2p^4\,{}^4P \rightarrow 2s^22p^3\,{}^4S^0$) from O^+ at the electron impact on O. The cross section for this emission is also shown in Fig. 6.1.

TABLE 6.1. Parameters in the extrapolation formula [Eq. (6.2)] for the energy distribution of secondary electrons at the ionization of O

Incident energy (eV)	A (eV)	B (10^{-18} cm^2/eV)
100	12.6	7.18
200	13.7	4.97
500	14.1	2.75
1000	14.0	1.69
2000	13.7	1.02

The energy distribution of the secondary (ejected and scattered) electrons is of practical importance. There is no measurement of the distribution reported for oxygen atoms. Burnett and Rountree[73] calculated the energy distribution, but only up to 30 eV of the energy (E_s) of the secondary electron. Here we fit the calculated result by a form

$$f(E_s) = \frac{B}{1+\left(\frac{E_s}{A}\right)^{\alpha}}. \tag{6.2}$$

We can produce a successful fit with the parameters $\alpha = 1.67$ and A and B shown in Table 6.1. The resulting distribution is plotted in Fig. 6.2. [Note that the Eq. (6.2) should be used only for the region $E_s < (E_e - I)/2$.] The reliability of the present distribution must be tested against experiment, however.

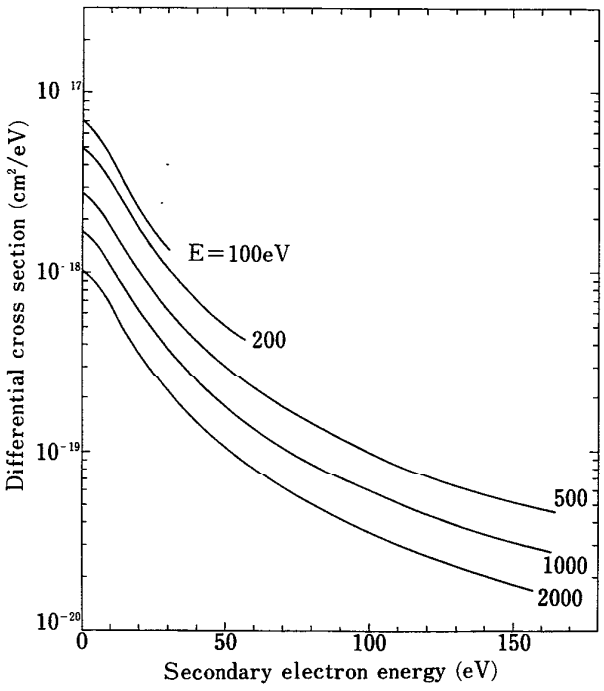

FIG. 6.2. Energy distribution of secondary electrons in the ionizing collision of electrons with O. Energy of the incident electron is indicated.

7. Electron Collisions: Attachment

Atomic oxygen can capture an electron to form a negative ion (O^-). There are two different processes for the electron attachment:

(i) radiative attachment

$$e + O \rightarrow O^- + h\nu, \tag{7.1}$$

(ii) three body attachment

$$e + e + O \rightarrow O^- + e. \tag{7.2}$$

It is very difficult to measure the cross section for any of the above two processes. We now have experimental information for the inverse of the processes; i.e.,

(iii) photodetachment

$$h\nu + O^- \rightarrow O + e, \tag{7.3}$$

(iv) electron-impact detachment

$$e + O^- \rightarrow O + e + e. \tag{7.4}$$

Using the principle of detailed balancing, we can deduce the cross section or the rate for processes (i) and (ii) from the corresponding quantities for (iii) and (iv).

Hoffmann[77] measured radiation (200–900 nm) emitted from an oxygen arc plasma at a temperature of ~9000 K. Assuming radiative equilibrium, he determined the absorption coefficient for the continuum radiation and therefrom the cross section for the photodetachment of O^-. From the photodetachment cross section, Hoffmann deduced the cross section for the attachment. The result is shown in Fig. 7.1. He indicated that the attachment cross section behaves as $E_e^{-0.6}$ in the region of low electron energy (E_e = 0.01 ~ 0.7 eV). He claimed ± 10% of uncertainty for his detachment cross section. Probably the attachment cross section in Fig. 7.1 includes a similar amount of error. It should be mentioned that the attachment cross section in Fig. 7.1 is in good agreement with the calculation by Garrett and Jackson.[78]

Peart *et al.*[79] reported their measurement of the cross section for the detachment process (7.4). Using the cross section and assuming a Maxwellian distribution of electron velocities, we calculate the rate constant for the electron detachment. Then the rate constant for the three-body attachment, $k_{3\text{-att}}$ is derived with the principle of detailed balancing. The resulting values are given in Fig. 7.2.

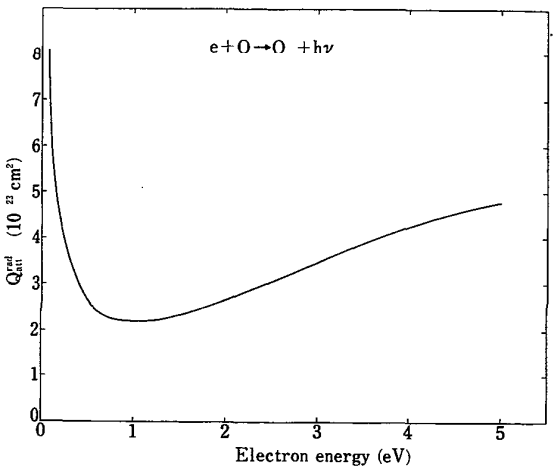

FIG. 7.1. Radiative attachment cross section for O, obtained by Hoffmann.[77]

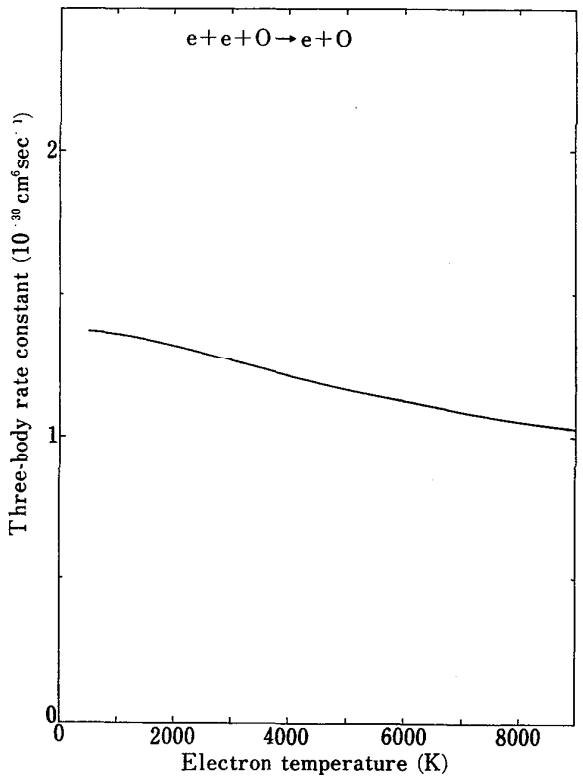

FIG. 7.2. Rate constant (in 10^{-30} cm^6 s^{-1}) for the three body attachment process ($e + e + O \rightarrow e + O^-$), derived from the corresponding quantity for the inverse process ($e + O^- \rightarrow e + e + O$).

There are a few problems encountered in the present method for deriving the $k_{3\text{-att}}$. Firstly, Peart *et al.* measured the detachment cross section only as low as 3.14 eV of electron energy. We extrapolated the cross section to the threshold (1.46 eV) using an analytical fit, to the measured values. In the fit, the data at lower energies have a much greater significance. These values, however, have a large uncertainty arising from the difficulty of the experiment. Thus the present rate constant shown in Fig. 7.2 has a large error (probably, a factor of 2 or more). Furthermore, in the above derivation, we had to ignore the fine structure of O and O^-. Thus the derived quantity is valid only in the temperature range shown in Fig. 7.2.

8. Summary and Future Problems

Cross sections for electron collisions with atomic oxygen are summarized in Fig. 8.1. The total-scattering cross section (Q_T) and the elastic cross section (Q_{elas}) are taken from Fig. 4.2, and the ionization cross section (Q_{ion}) from Fig. 6.1. In addition, cross sections are presented for a num-

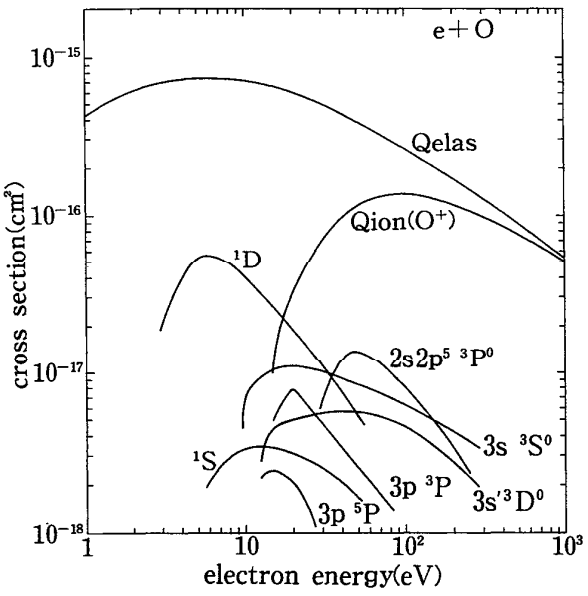

FIG. 8.1. Summary of the cross sections for the electron collision with atomic oxygen. Representative data are reproduced from the figures in the previous sections. All the processes having a relatively large cross section are shown except for the excitation of $3s''\ ^3P^0$ state. That excitation has a cross section of magnitude similar to the excitation of $2s2p^5\ ^3P^0$ state.

ber of representative excitation processes described in Sec. 5. For these cross sections, experimental values which we smoothly connected are plotted in Fig. 8.1.

Collisions of atomic oxygen with electrons and photons are now quite well understood, if we take into account the difficulty in handling oxygen atoms both experimentally and theoretically. Atomic oxygen is not only of significance in applications but is also of interest in atomic physics. It is, for instance, one of the typical examples of open-shell atoms, which behave differently from the closed-shell atoms like rare gases. Thus more work is required on the collisions between atomic oxygen and electrons or photons. Some examples of future problems are

(i) More elaborate and quantitative experimental determinations of Q_T and Q_{elas} are needed. These two cross sections can serve as a standard to which cross sections for any other processes may be compared.

(ii) A more detailed comparison should be made among the experimental and theoretic cross sections for the excitation of the $2p^4\ ^1D$ and ^1S states, so that the best reliable data for those cross sections will be established.

(iii) As is shown in Sec. 5, experimental data are now available for various excitation processes in the collision, $e + O$. These data, however, include a large uncertainty and, in many cases, exist only at a few point of collision energy. More refined and more extensive measurement would be highly desirable. For some of the excitation processes, results of rather comprehensive calculations are now available. The theoretic cross section, however, cannot necessarily reproduce the experimental value.

(iv) In practical applications, emission cross sections Q_{emis} are quite useful. As is seen in Section 5.4, however, the measured values of Q_{emis} are sometimes inconsistent with those of Q_{exc}. A further study is necessary to solve this discrepancy.

(v) There is no measurement of the cross section for the production of ions in their specific state upon electron collisions. Also, any measurement of the energy distribution of the secondary electrons should be made at the electron-impact ionization of O.

(vi) Electron or photon collisions with oxygen atoms in their excited state (metastable states, in particular) are of importance, but no reliable data are as yet available.

9. Acknowledgments

During the course of the present data compilation, many colleagues provided us with information about the data shown here. Particular thanks are due to Prof. J. P. Doering and Drs. K. A. Berrington and S. S. Tayal, who sent us their cross sections prior to publication.

10. References

[1]Y. Itikawa, M. Hayashi, A. Ichimura, K. Onda, K. Sakimoto, K. Takayanagi, M. Nakamura, H. Nishimura, and T. Takayanagi, J. Phys. Chem. Ref. Data **15**, 985 (1986).
[2]Y. Itikawa, A. Ichimura, K. Onda, K. Sakimoto, K. Takayanagi, Y. Hatano, M. Hayashi, H. Nishimura, and S. Tsurubuchi, J. Phys. Chem. Ref. Data **18**, 23 (1989).
[3]Y. Itikawa, S. Hara, T. Kato, S. Nakazaki, M. S. Pindzola, and D. H. Crandall, Atomic Data Nucl. Data Tables **33**, 149 (1985).
[4]K. L. Bell, H. B. Gilbody, J. G. Hughes, A. E. Kingston, and F. J. Smith, J. Phys. Chem. Ref. Data **12**, 891 (1983).
[5]C. E. Moore, *Selected Tables of Atomic Spectra, Atomic Energy Levels and Multiplet Tables*, O I, NSRDS-NBS **3**, Sec. 7 (1976).
[6]S. Bashkin and J. O. Stoner, Jr., *Atomic Energy Levels and Grotrian Diagrams* (North-Holland, Amsterdam, 1975), Vol. I.
[7]P. M. Dehmer, J. Berkowitz, and W. A. Chupka, J. Chem. Phys. **59**, 5777 (1973).
[8]D. M. Neumark, K. R. Lykke, T. Andersen, and W. C. Lineberger, Phys. Rev. A **32**, 1890 (1985).
[9]J. P. Doering, E. E. Gulcicek, and S. O. Vaughan, J. Geophys. Res. **90**, 5279 (1985).
[10]W. L. Wiese, M. W. Smith, and B. M. Glennon, *Atomic Transition Probabilities*, NSRDS-NBS 4 (1966), Vol. I, H through Ne.
[11]D. B. Jenkins, J. Quant. Spectrosc. Radiat. Transfer **34**, 55 (1985).
[12]A. K. Pradhan and H. E. Saraph, J. Phys. B **10**, 3365 (1977).
[13]P. M. Dehmer, W. L. Luken, and W. A. Chupka, J. Chem. Phys. **67**, 195 (1977).
[14]W. L. Luken and O. Sinanoglu, J. Chem. Phys. **64**, 1495 (1976).
[15]E. J. Knystautas, M. Brochu, and R. Drouin, Can. J. Spectrosc. **18**, 143 (1973).
[16]W. H. Smith, J. Bromander, L. J. Curtis, H. G. Berry, and R. Buchta, Astrophys. J. **165**, 217 (1971).
[17]K. L. Baluja and C. J. Zeippen, J. Phys. B **21**, 1455 (1988).
[18]C. Froese Fischer and H. P. Saha, Phys. Rev. A **28**, 3169 (1983).
[19]C. J. Zeippen, M. J. Seaton, and D. C. Morton, Mon. Not. R. Astr. Soc. **181**, 527 (1977).
[20]R. R. Teachout and R. T. Pack, Atomic Data **3**, 195 (1971).
[21]R. A. Alpher and D. R. White, Phys. Fluids **2**, 153 (1959).
[22]H.-J. Werner and W. Meyer, Phys. Rev. A **13**, 13 (1976).
[23]J. L. Dehmer, M. Inokuti, and R. P. Saxon, Phys. Rev. A **12**, 102 (1975).
[24]M. Inokuti, T. Baer, and J. L. Dehmer, Phys. Rev. A **17**, 1229 (1978).
[25]G. D. Zeiss, W. J. Meath, J. C. F. MacDonald, and D. J. Dawson, Can. J. Phys. **55**, 2080 (1977).
[26]M. J. Seaton, in *Recent Studies in Atomic and Molecular Processes*, edited by A. E. Kingston (Plenum, 1987), p. 29.

[27]J. A. R. Samson and P. N. Pareek, Phys. Rev. A **31**, 1470 (1985).
[28]G. C. Angel and J. A. R. Samson, Phys. Rev. A **38**, 5578 (1988).
[29]K. Kirby, E. R. Constantinides, S. Babeu, M. Oppenheimer, and G. A. Victor, Atomic Data Nucl. Data Tables **23**, 63 (1979).
[30]J. A. R. Samson and V. E. Petrosky, Phys. Rev. A **9**, 2449 (1974).
[31]J. L. Dehmer and P. M. Dehmer, J. Chem. Phys. **67**, 1782 (1977).
[32]M. I. A. Hussein, D. M. P. Holland, K. Codling, P. R. Woodruff, and E. Ishiguro, J. Phys. B **18**, 2827 (1985).
[33]A. K. Pradhan, J. Phys. B **11**, L729 (1978).
[34]B. L. Henke, P. Lee, T. J. Tanaka, R. L. Shimabukuro, and B. K. Fujikawa, Atomic Data Nucl. Data Tables **27**, 1 (1982).
[35]R. C. Dehmel, M. A. Fineman, and D. R. Miller, Phys. Rev. A **13**, 115 (1976).
[36]G. Sunshine, B. B. Aubrey, and B. Bederson, Phys. Rev. **154**, 1 (1967).
[37]Vo Ky Lan, N. Feautrier, M. Le Dourneuf, and H. van Regemorter, J. Phys. B **5**, 1506 (1972).
[38]S. P. Rountree, E. R. Smith, and R. J. W. Henry, J. Phys. B **7**, L167 (1974).
[39]L. D. Thomas and R. K. Nesbet, Phys. Rev. A **11**, 170 (1975).
[40]L. D. Thomas and R. K. Nesbet, Phys. Rev. A **12**, 1729 (1975).
[41]B. R. Tambe and R. J. W. Henry, Phys. Rev. A **13**, 224 (1976).
[42]B. R. Tambe and R. J. W. Henry, Phys. Rev. A **14**, 512 (1976).
[43]M. Blaha and J. Davis, Phys. Rev. A **12**, 2319 (1975).
[44]M. E. Riley, C. J. MacCallum, and F. Biggs, Atomic Data Nucl. Data Tables **15**, 443 (1975).
[45]H. C. Carlson, Jr. and G. P. Mantas, J. Geophys. Res. **87**, 4515 (1982).
[46]E. L. Breig and C. C. Lin, Phys. Rev. **151**, 67 (1966).
[47]H. E. Saraph, J. Phys. B **6**, L243 (1973).
[48]B. R. Tambe and R. J. W. Henry, Phys. Rev. A **10**, 2085 (1974).
[49]M. Le Dourneuf and R. K. Nesbet, J. Phys. B **9**, L241 (1976).
[50]K. A. Berrington, J. Phys. B **21**, 1083 (1988).
[51]T. W. Shyn and W. E. Sharp, Geophys. Res. Lett. **12**, 171 (1985).
[52]T. W. Shyn and W. E. Sharp, J. Geophys. Res. **91**, 1691 (1986).
[53]T. W. Shyn, S. Y. Cho, and W. E. Sharp, J. Geophys. Res. **91**, 13751 (1986).
[54]J. P. Doering and E. E. Glucicek, J. Geophys. Res. **94**, 1541 (1989).
[55]K. A. Berrington and P. G. Burke, Planet. Space Sci. **29**, 377 (1981).
[56]R. J. W. Henry, P.G. Burke, and A. L. Sinfailam, Phys. Rev. **178**, 218 (1969).
[57]E. R. Smith, Phys. Rev. A **13**, 65 (1976).
[58]S. S. Tayal and R. J. W. Henry, Phys. Rev. A **38**, 5945 (1988).
[59]S. S. Tayal and R. J. W. Henry, Phys. Rev. A **39**, 4531 (1989).
[60]S. O. Vaughan and J. P. Doering, J. Geophys. Res. **92**, 7749 (1987).
[61]S. O. Vaughan and J. P. Doering, J. Geophys. Res. **91**, 13755 (1986).
[62]E. E. Gulcicek and J. P. Doering, J. Geophys. Res. **93**, 5879 (1988).
[63]S. O. Vaughan and J. P. Doering, J. Geophys. Res. **93**, 289 (1988).
[64]E. E. Gulcicek, J. P. Doering, and S. O. Vaughan, J. Geophys. Res. **93**, 5885 (1988).
[65]T. Sawada and P. S. Ganas, Phys. Rev. A **7**, 617 (1973).
[66]J. P. Doering and E. E. Gulcicek, J. Geophys. Res. **94**, 2733 (1989).
[67]S. P. Rountree, J. Phys. B **10**, 2719 (1977).
[68]E. C. Zipf and P. W. Erdman, J. Geophys. Res. **90**, 11087 (1985).
[69]E. C. Zipf and W. W. Kao, Chem. Phys. Lett. **125**, 394 (1986).
[70]E. J. Stone and E. C. Zipf, J. Chem. Phys. **60**, 4237 (1974).
[71]G. A. Germany, R. J. Anderson, and G. J. Salamo, J. Chem. Phys. **89**, 1999 (1988).
[72]E. Brook, M. F. A. Harrison, and A. C. H. Smith, J. Phys. B **11**, 3115 (1978).
[73]T. Burnett and S. P. Rountree, Phys. Rev. A **20**, 1468 (1979).
[74]D. L. Ziegler, J. H. Newman, K. A. Smith, and R. F. Stebbings, Planet. Space Sci. **30**, 451 (1982).
[75]E. C. Zipf, Planet. Space Sci. **33**, 1303 (1985).
[76]E. C. Zipf, W. W. Kao, and R. W. McLaughlin, Chem. Phys. Lett. **118**, 591 (1985).
[77]H. Hoffmann, J. Quant. Spectrosc. Radiat. Transfer **21**, 163 (1979).
[78]W. R. Garrett and H. T. Jackson, Jr., Phys. Rev. **153**, 28 (1967).
[79]B. Peart, R. A. Forrest, and K. Dolder, J. Phys. B. **12**, 2735 (1979).
[80]A. Corney and O. M. Williams, J. Phys. B **5**, 686 (1972).
[81]J. A. Kernahan and P.H-L. Pang, Can. J. Phys. **53**, 455 (1975).